Electronic Supplementary Material (ESM)

The GLP-1 analogue lixisenatide decreases atherosclerosis in insulin-resistant mice by modulating macrophage phenotype

Ángela Vinué[1], Jorge Navarro[1,2,3], Andrea Herrero-Cervera[1], Marta García-Cubas[1], Irene Andrés-Blasco[1], Sergio Martínez-Hervás[1,4,5] José T. Real[1,4,5], Juan F. Ascaso[1,4,5] and Herminia González-Navarro[1,5]

1. Institute of Health Research-INCLIVA, Avda Menéndez Pelayo 4, 46010 Valencia, Spain

2. Clinic Hospital and Department of Medicine, University of Valencia, Institute of Health Research-INCLIVA, Valencia, Spain

3. CIBER Epidemiologia y Salud Pública (CIBERESP), Madrid, Spain

4. Endocrinology and Nutrition Department, Clinic Hospital and Department of Medicine, University of Valencia, Valencia, Spain

5. Centro de Investigación Biomédica en Red de Diabetes y Enfermedades Metabólicas Asociadas (CIBERDEM), Madrid, Spain

Ángela Vinué and Jorge Navarro contributed equally to this work.

Corresponding author

H. González-Navarro, Institute of Health Research-INCLIVA, Avda Menéndez Pelayo 4, 46010 Valencia, Spain

E-mail: herminia.gonzalez@uv.es

Methods

Metabolic measurements in mice Glucose tolerance tests (GTT) were performed by intraperitoneal injection of glucose (2 g/Kg of body weight, BW) in overnight-fasted mice and plasma glucose and insulin levels were analyzed at different time-points using a glucometer (Ascensia Elite, Bayer, Sant Joan Despí, Spain) and an ultrasensitive anti-mouse insulin ELISA kit (Mercodia, Uppsala, Sweden) [1]. Insulin tolerance tests (ITT) were performed in 4h-fasted mice by intraperitoneal injection of insulin (0.5 U/Kg of BW Humulina, Lilly, Alcobendas, Spain) and glucose levels were measured at different time-points [2].

Immunohistopathological analysis of atheromas The Masson's trichrome staining was used to determine the collagen content, necrotic core area, and fibrous cap thickness of aortic cross-sections; the necrotic cores were defined as non-stained acellular areas and, for the fibrous cap thickness, an average of 3-5 values for regions above the necrotic cores was used [3]. The atheroma macrophage content was detected with a rat anti-Mac-3 monoclonal antibody (1/200, sc-19991, Santa Cruz Biotechnology, Santa Cruz, CA, USA) followed by a biotin-conjugated goat anti-rat secondary antibody (1/300, sc-2041, Santa Cruz), streptavidin-HRP (TS-060-HR, LabVision, Fremont, CA, USA), and DAB substrate (SK4100, Vector Laboratories, Burlingame, CA; USA). For MMP-9, iNOS and arginase I immunohistochemistry, sections were treated for antigen retrieval (citrate buffer, 10 mM, pH 6.5 high pressure and temperature) followed by peroxidase inactivation (H_2O_2 3%), blocking with horse serum (5%), incubation overnight at 4° C with primary antibodies (rabbit anti-MMP-9,

1/200 dilution, [AB19016, UPSTATE-Millipore, Billerica, MA, USA], anti-iNOS antibody 1/100 [ab15323, Abcam, Cambridge, UK], and anti-arginase I 1/50, [AV45673, Sigma, St. Louis, MO, USA]), incubation with a biotinylated anti-rabbit secondary antibody (1/500 dilution, sc-2040 Santa Cruz), streptavidin-HRP and DAB substrate. Slides counterstained with hematoxylin were mounted with EUKITT (A10500, Deltalab, Barcelona, Spain). VSMC content was determined using an anti-SMα-actin monoclonal alkaline phosphatase-conjugated antibody (1/20 dilution, a-5691, Sigma) and developed using Fast Red substrate (Sigma). Slides were mounted with glycerol gelatin (Sigma). Images were captured with an OPTIKAMPRO5 digital camera mounted on a stereo microscope (Optika, Ponteranica, Italy). T-lymphocytes in atheromas were detected by immunofluorescence using a polyclonal anti-human CD3 antibody (1/75, A0452, Dako, Santa Clara, CA, USA) and Alexa Fluor®-488 anti-rabbit IgG secondary antibody (1/200, Invitrogen, Life Technologies, Thermofisher Scientific, Madrid, Spain). Slides were mounted with Slow-Fade Gold reagent (S36936, Invitrogen) and analyzed with an inverted fluorescent microscope (DMI3000B, Leica, Wetzlar, Germany).

Double immunofluorescence of Mac-3/iNOS and Mac-3/ArgI included antigen retrieval with sodium citrate buffer as before, followed by blocking (5% vol/vol horse serum, 1h at RT), incubation (overnight at 4° C) with primary antibodies overnight at 4 ºC (a rabbit polyclonal anti-iNOS antibody [1/50, ab 15323, Abcam] or a rabbit polyclonal anti-arginase I antibody [1/50, AV45673, Sigma] combined with a rat monoclonal anti-Mac3 antibody [1/200, sc-19991, Santa Cruz]) and by incubation (1h at RT) with a goat anti-rat IgM Alexa Fluor®-594 and anti-rabbit IgG Alexa Fluor®-488 secondary antibodies (A21213 and A11034, Invitrogen). Nuclear staining was performed with 4',6-

diamidino-2-phenylindole (DAPI; D1306, Thermofisher Scientific). Slides were mounted with Slow-Fade and analyzed as before [3].

Proliferation and apoptosis of macrophages inside the lesions were determined by double immunofluorescence of Ki67/F4/80 and CL (cleaved)-caspase 3/F4/80 which included antigen retrieval with sodium citrate buffer as above, followed by blocking as before, incubation (overnight at 4° C) with primary antibodies (a rabbit monoclonal anti-Ki67 antibody [clone SP6, MAD-000310QD, VITRO, Madrid, Spain] combined with a rat anti-F4-80 1/50 antibody [MCA497G AbD Serotec, BioRad, Hercules, CA, USA], a rabbit anti-CL-caspase-3 [D175; 1/200, 9661 Cell Signaling] antibody, or a rat anti-F4-80 antibody) and by incubation (1h at RT) with a goat anti-rat IgM Alexa Fluor®-594 and anti-rabbit IgG Alexa Fluor®-488 secondary antibodies (Invitrogen). For the apoptosis studies nuclear staining was also performed with DAPI. Slides were mounted and analysed as above.

All antibodies used for immunohistochemistry and immunofluorescence were validated by performing negative controls by omitting primary antibodies or adding irrelevant antibodies.

Flow cytometry measurements For circulating leukocyte analysis, 10 µl of heparinised whole blood was incubated for 30 min at RT with CD45-FITC (BD Pharmingen, Madrid, Spain), Ly6C-PerCP (BD Pharmingen) and CD115-APC (BioLegend, San Diego, CA, USA) antibodies or with 5 µl Brilliant Stain Buffer (BD) and the following antibodies (BD): rat anti-mouse CD4-BV, rat anti-mouse CD8a-BV, anti-mouse CD69-PE or anti-mouse CD3e-APC. The samples were incubated with lysing solution prior to flow cytometry analysis (FACSVerse Flow cytometer, BD). $Ly6C^{low}$-, $Ly6C^{int}$- and $Ly6C^{hi}$-monocyte subsets were determined in CD115+ populations as described [4]. Leukocytes were identified as CD45+ cells, lymphocytes and neutrophils by

morphology and monocytes by the CD115 marker. All antibodies used for flow cytometry were validated by Flow cytometry core.

Western blot analysis Protein extracts were obtained by homogenising cellular pellets of macrophages in the presence of ice-cold lysis TNG buffer (Tris-HCl 50 mM, pH 7.5, NaCl 200 mM, Tween-20 1% vol/vol, NP-40 0.2% vol/vol) supplemented with Complete Mini cocktail, PhosSTOP (Roche, Mannheim, Germany), beta-glycerophosphate 50 mM (Sigma), 2 mM phenylmethylsulfonyl fluoride (PMSF, Roche) and 200 µM Na_3VO_4 (Sigma). For protein analysis, protein extracts (35-50 µg) were prepared with Laemmli buffer (5 min 95° C) and subjected to 12% w/v polyacrylamide gel electrophoresis and western blot as described [2]. The following primary (1/200) and secondary (1/2000) antibodies were used to detect the proteins: anti-phosphoSer727-STAT1 (07-714, Millipore), anti-STAT1(sc-346, Santa Cruz Biotechnology, Santa Cruz, CA, USA), anti-phosphoTyr705-STAT3 (9131, Cell Signaling, Danvers, MA, USA), anti-STAT3 (sc-8019 Santa Cruz), anti-phosphop38 (sc-17852, Santa Cruz), anti-p38 (sc-535, Santa Cruz), anti-phosphoERK (sc-7383 SantaCruz), anti-ERK (sc-154 SantaCruz), anti-arginase I (AV45673, Sigma), anti-iNOS (15323, Abcam), anti-α-tubulin (sc-8035, SantaCruz), anti-phosphoSAPK/JNK (9251 Cell Signaling), anti-SAPK/JNK (9258 Cell Signaling), anti-mouse IgG-HRP (sc-2005) and goat anti-rabbit IgG-HRP (sc-2004). The immunocomplexes were detected with an ECL Plus detection kit (ThermoFisher). All antibodies for western blot were acquired and used after checking that validation was performed by manufacturer company.

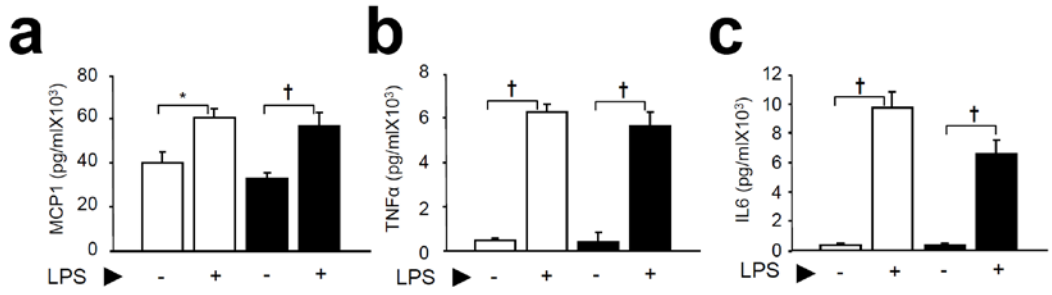

ESM-Fig. 1. Cytokine secretion in *apoE-/-Irs2+/-* mouse macrophages treated with lixisenatide. Secretion of inflammatory **(a)** MCP1, **(b)** TNFα, and **(c)** IL6 cytokines in *apoE-/-Irs2+/-* macrophages treated with 40 nM Lixi or vehicle in basal conditions and stimulated with LPS (100 ng/ml) for 24 h. Statistical analysis was performed using one-way ANOVA test followed by Tukey's post hoc test. White bars vehicle-treated macrophages; black bars Lixi-treated macrophages. *p<0.01,†p<0.001. (n=8).

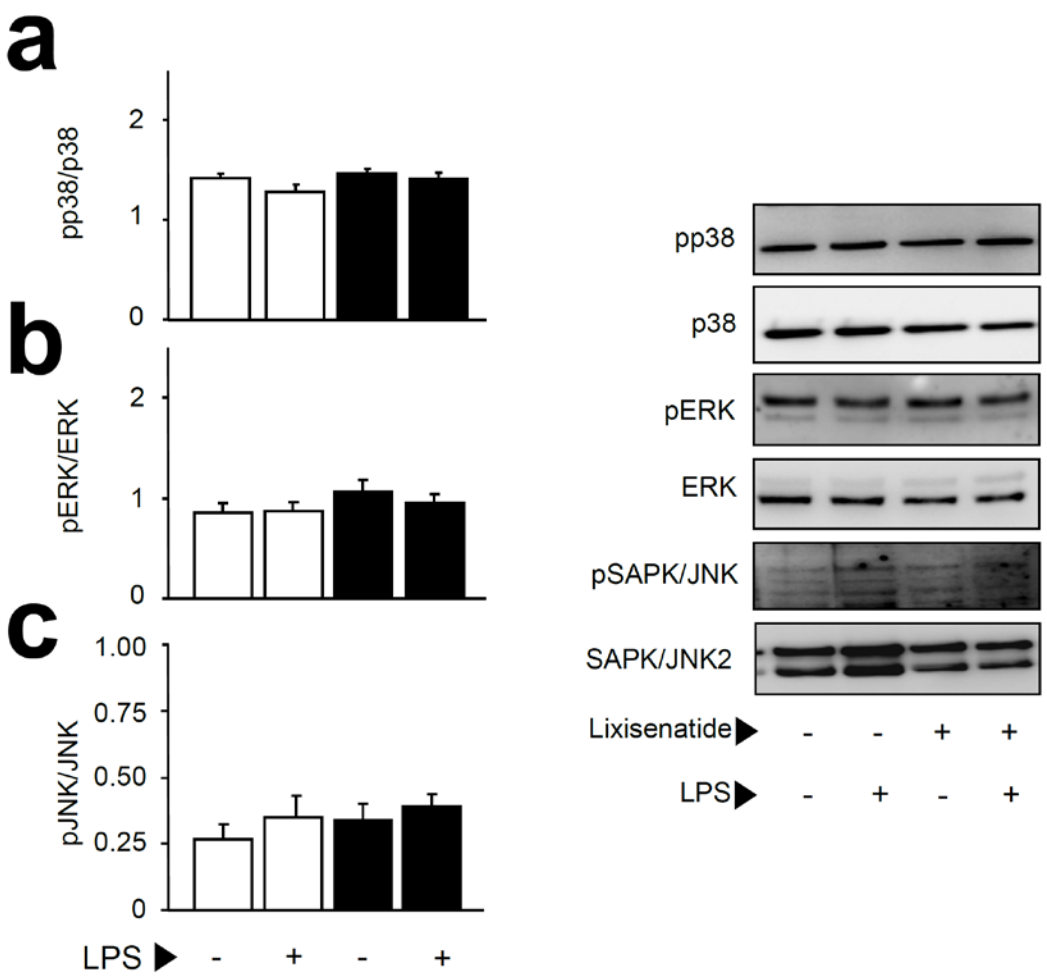

ESM-Fig. 2. Activation of the MAPKinases in mouse *apoE-/-Irs2+/-* macrophages differentiated in the presence of lixisenatide or vehicle. Protein analysis of the activated (phosphorylated) and total forms of **(a)** p38, **(b)** ERK and **(c)** SAPK/JNK in macrophages differentiated with 40 nM Lixi or vehicle and then stimulated or not with LPS (100 ng/ml) during 6h. For quantification phosphorylated forms were normalized to total p38, total ERK and SAPK/JNK levels. Representative blots of the phosphorylated and unphosphorylated forms of the different proteins analyzed are shown. Statistical analysis was performed using one-way ANOVA test followed by Tukey's post hoc test. White bars vehicle-treated macrophages; black bars Lixi-treated macrophages. (*n*=3-5).

References

[1] Gonzalez-Navarro H, Vinue A, Sanz MJ, et al. (2013) Increased dosage of Ink4/Arf protects against glucose intolerance and insulin resistance associated with aging. Aging Cell 12: 102-111

[2] Vinue A, Andres-Blasco I, Herrero-Cervera A, et al. (2015) Ink4/Arf locus restores glucose tolerance and insulin sensitivity by reducing hepatic steatosis and inflammation in mice with impaired IRS2-dependent signalling. Biochim Biophys Acta 1852: 1729-1742

[3] Martinez-Hervas S, Vinue A, Nunez L, et al. (2014) Insulin resistance aggravates atherosclerosis by reducing vascular smooth muscle cell survival and increasing CX3CL1/CX3CR1 axis. Cardiovasc Res 103: 324-336

[4] Andres-Blasco I, Vinue A, Herrero-Cervera A, et al. (2016) Hepatic lipase inactivation decreases atherosclerosis in insulin resistance by reducing LIGHT/Lymphotoxin beta-Receptor pathway. Thromb Haemost 116: 379-393